Fermilab Proposal No. 439

Scientific Spokesman

D. Garelick
Physics Department
Northeastern University
Boston, Mass. 02115

PH: 617 - 437-2936

High Sensitivity Search for New States Which Decay into Muons

D. Garelick, P. Gauthier, M. Glaubman, J. Johnson
M. Mallary, E. Pothier, D. Potter, M. Ronan, E. von Goeler

Northeastern University

September 20, 1975

FNAL proposal # 439

High Sensitivity Search for New States Which Decay into Muons

D. Garelick*, P. Gauthier, M. Glaubman,
J. Johnson, M. Mallary, E. Pothier, D. Potter, M. Ronan,
E. von Goeler

Northeastern University, Boston, Mass. 02115

(September 20, 1975)

*Spokesman Telephone (617)-437-2936

Abstract

The reaction p + Fe→muons + anything will be measured to search for new states in the 3.0 to 25.0 GeV mass region which decay into two or more muons. A beam dump method will be used with a beam of 400 GeV protons at an intensity of $\sim 10^9$ protons per pulse. In 300 hours of data taking, new states with $\sigma B \sim 10^{-38}$ cm^2 per nucleon will appear as a 5 standard deviation effect (~ 25 events, assuming $\sim$ zero background).

Introduction

The recent indication of the existence of a heavy lepton[1] has led theorists[2] to "predict" new narrow resonances which decay into $\mu^+\mu^-$. We propose here[3] a conceptually simple but extremely sensitive experiment to see whether or not such states exist.

In addition, we will collect three and four muon events. For example, such events could be caused by particles, χ, whose dominant decay is $\chi \to \gamma\psi$. Such states will also have decays of the type $\chi \to 4\mu$. Another example is a possible excited state of the μ whose dominant decay is $\mu^* \to \gamma\mu$ which will also have decays of the type $\mu^* \to 3\mu$.

The Technique

At 400 GeV, $\gamma_{cm} = 14.6$. Thus, any apparatus which is to detect muon states produced at rest in the c. m. system must subtend lab angles of at least $\pm$ 68 m rad. The proposed detector, Fig. 1, subtends $\pm$ 100 m rad. As an example of the detection efficiency, particles produced at rest in the c. m. system which decay into $\mu^+\mu^-$ have a detection efficiency of $\sim$36%.

As indicated in Fig. 1, the detector is divided into two halves. Each half consists of 10 scintillation counters for triggering and 4 banks of drift chambers[4] for measuring the muon trajectories[5]. The detector has been divided into halves in a way which allows a center vertical

strip of the detector to be deactivated[6]. This allows for the suppression of backgrounds from unwanted low mass pairs produced along the beam direction ($\sim 3 \times 10^3$ per pulse at 10^9 p/ pulse) and from beam muons. For purposes of calibrations, the center strip will be made active. During data runs, events in which two or more μ's are detected will be recorded ($\sim$ 300 per pulse at $\sim 10^9$ p/ pulse).

Our past experience[5] indicates that the proposed apparatus will probably be background limited[7] at fluxes of $\sim 10^{9\pm1}$ protons/ pulse. We will run at as high a beam flux as possible and plan to spend the first 200 hours of beam time optimizing and calibrating the apparatus.

For an incident flux of 10^9 p/ pulse we estimate that a new state with $\sigma B \sim 10^{-38}$ cm^2 per nucleon will appear as a 5 standard deviation effect.

The mass resolution[3,5] of the apparatus is $\delta M/M \sim \pm 10\%$.

Requirements

We hope FNAL will supply: 1) the magnets;[8] 2) drift chamber electronics for $\sim$600 sense wires; 3) fast electronics for triggering and monitoring purposes; 4) a beam of variable intensity between 10^7 and 10^{10} protons per pulse; 5) approximately 100 hours of FNAL-CDC-6600 time for checking the performance of the apparatus; 6) Beam time: 200 hours tests and calibrations and 300 hours of data.

We will supply: 1) the drift chambers; 2) trigger counters; 3) data logging computer.

Scheduling

The experiment could begin as early as June, 1976. The actual starting date will depend on the schedule for approved experiments #411 and #413. (Note: The detector proposed here could also serve as an excellent μ detector for experiments #411 and #413. Thus, a meshing of this experiment with the other experiments appears quite feasible.)

Footnotes

(1) M. Perl, et al., Lepton/ Photon Conf., Aug.,1975.

(2) H. Harari, Lepton/ Photon Conf., Aug.,1975

(3) This proposal is an update of a proposal called "365F" which was presented to the PAC by the Northeastern High Energy Group, Mar.20, 1975. (see, Request for Additional Accelerator Time, Fermilab Experiment #365, Northeastern High Energy Experimental Group, Mar.18, 1975).

(4) Proportional chambers are also being considered.

(5) For a description of the beam dump technique, see: G. J. Blanar, et al., Phys. Rev. Lett. 35, 346(1975) and G. J. Blanar, et al., SLAC Topical Conference, July, 1975 (to be published). These references are attached to this proposal.

(6) The actual width of this strip will be determined by the backgrounds encountered.

(7) We have taken good data at 10^7 protons/ pulse with a simular apparatus (Experiment #365) which used spark chambers as the detectors.

(8) The $2' \times 2' \times 10'$ and the $3' \times 3' \times 4'$ magnets are of the "Genesis" type built for Experiment #365.

FIG. 1

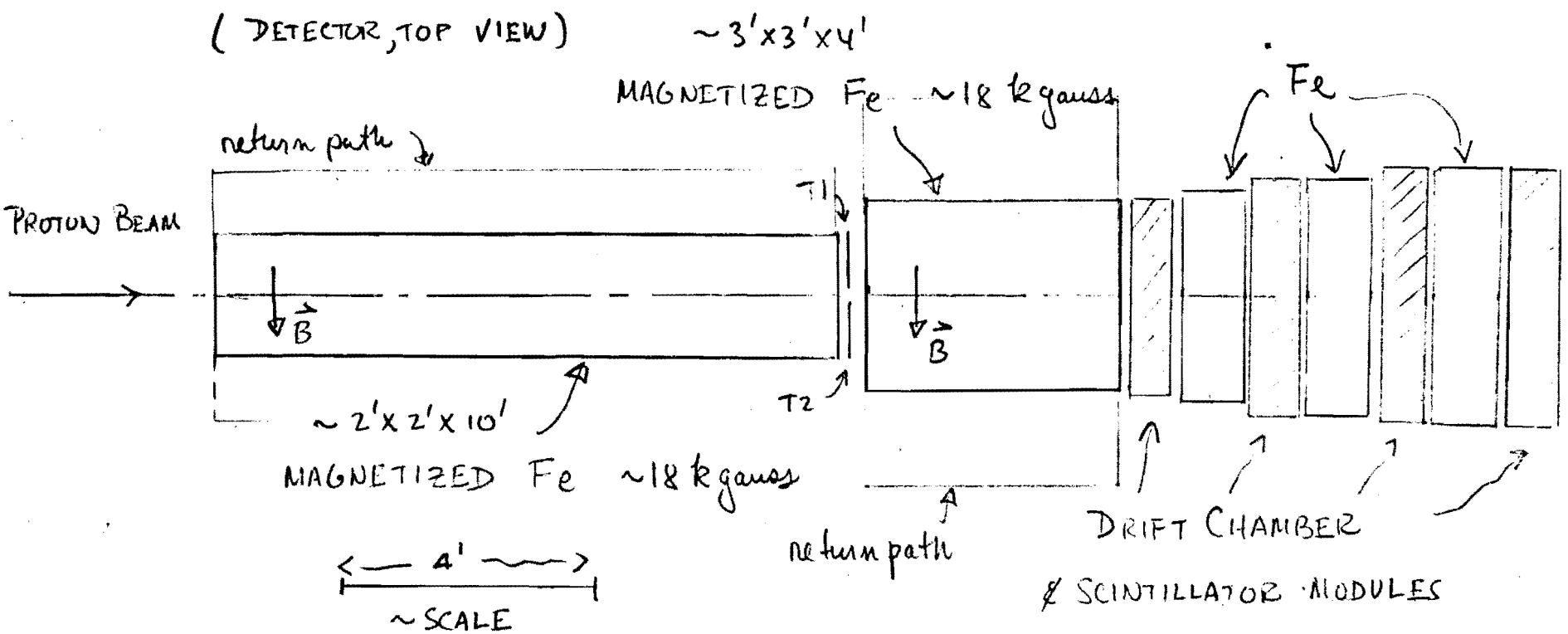

TYPICAL DRIFT CHAMBER & SCINTILLATOR MODULE 4'x4'
(48 vertical cells 4'x2" & 96 horizontal (and tilted) cells 2'x2")
total system ≃ 600 sense wires

Measurement of $\psi(3.1)$ Meson Production by Pions and Protons*†

G. J. Blanar, C. F. Boyer, W. L. Faissler, D. A. Garelick,‡ M. W. Gettner, M. J. Glaubman, J. R. Johnson, H. Johnstad, M. L. Mallary, E. L. Pothier, D. M. Potter, M. T. Ronan, M. F. Tautz, E. von Goeler, and Roy Weinstein
Northeastern University at Boston, Boston, Massachusetts 02115
(Received 14 July 1975)

The production of $\psi(3.1)$ mesons is reported for the reactions $\pi^- + \mathrm{Fe} \to \mu^+ + \mu^- +$ anything, at 200 GeV, and $p + \mathrm{Fe} \to \mu^+ + \mu^- +$ anything, at 240 GeV. For ψ production, distributions in $x \equiv P_L/P_{\mathrm{beam}}$ and $P_\perp$ are given. For $x \geq 0.5$, the ratio of the ψ production cross sections in iron for pions to that for protons is found to be 7.4 ± 2.0.

We report here results of an experiment carried out at the Fermi National Accelerator Laboratory (FNAL) in which enhancements are observed in the dimuon invariant-mass spectra at about 3.1 GeV. The reactions studied were

$$\pi^- + \mathrm{Fe} \to \mu^+ + \mu^- + \text{anything}, \quad P_B = 200 \text{ GeV}, \quad (1)$$

and

$$p + \mathrm{Fe} \to \mu^+ + \mu^- \text{ anything}, \quad P_B = 240 \text{ GeV}, \quad (2)$$

where P_B is the monoenergetic beam momentum. We interpret the enhancements, whose widths are consistent with the resolution of our apparatus, as the $\psi(3.1)$ meson.[1]

The μ-pair detector is shown in Fig. 1(a). The μ pairs were created at the front end of the first iron (Fe) absorber. Muons were identified by their traversal of 5.6 m of Fe. Muon momenta and angles were measured using a 56-kG-m gapless magnet and associated wire-chamber system.

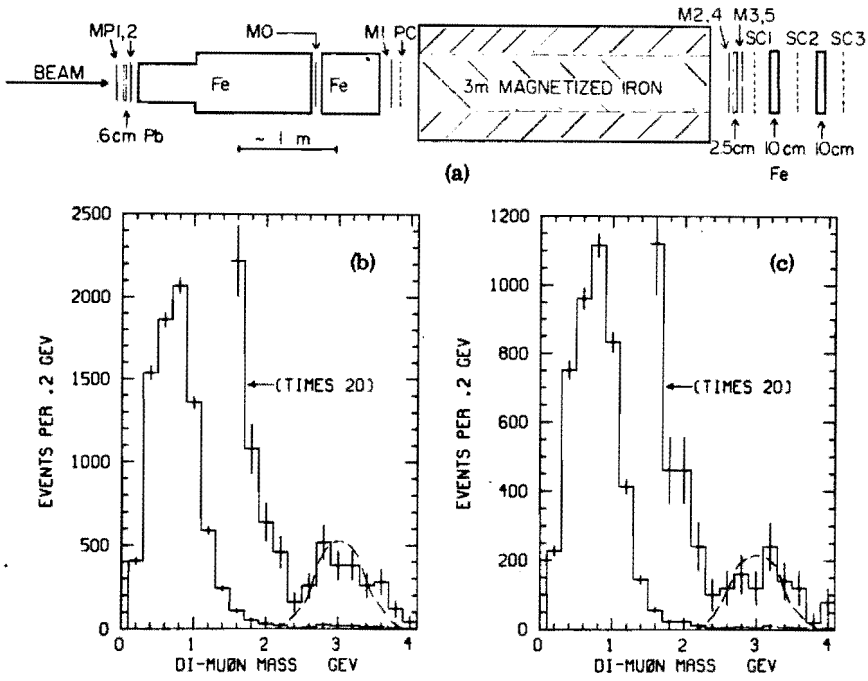

FIG. 1. (a) Muon-pair detector (top view). SC ≡ spark chamber; M ≡ scintillation counter; PC ≡ proportional chamber; SC2 limits the vertical aperture to ± 24 cm. (b),(c) Dimuon invariant-mass spectra for Reactions (1) (pion beam) and (2) (proton beam), respectively.

Events were recorded whenever there was a six-fold counter coincidence, M0·M1·(M2·M3)·(M4·M5), in time with a beam particle defined by scintillation counters and hodoscopes (not shown). The split-counter coincidence, (M2·M3)·(M4·M5), required that there be at least two particles at the rear of the magnet. For each event, coordinates from the chambers, counter tags, and pulse heights from counters MP1, MP2, M0, M1, two beam Cherenkov counters, and the final beam-defining counter were recorded.

The dimuon invariant mass was calculated from the tracks measured by the spark chambers, under the assumption that the dimuon was created inside the first Fe absorber 12.7 cm from its front edge along the beam line. The muon momenta and angles were reconstructed by taking into account the bending and energy loss of the muons in the magnetized Fe spectrometer. The proportional chamber was used only in checking the reconstruction technique and the spark-chamber efficiencies for a subsample of the data.

The reconstruction process selected μ pairs for which the total charge was zero. This eliminated $\approx 2\%$ of the 2μ events. Also, in the horizontal-plane projection, where there is no bending, each muon track was extrapolated back to the region of the production point. In this region, the tracks were required to deviate horizontally from the production point by less than 2.2 times the expected standard deviation. The standard deviation, Δ, was calculated from the bending of the muon in the vertical plane (muon momentum) and the expected multiple scattering of the muon in the spectrometer. (At 100 GeV, $\Delta = 1$ cm.) This requirement removed $\approx 10\%$ of the events. For the accepted events, the distribution of the track positions at the production point agreed well with the distribution calculated from the properties of the spectrometer. Monoenergetic muon beams with energies of approximately 100 and 200 GeV were used to calibrate and check the spectrometer and measure its resolution. Also, counters MP1 and MP2 were used to show that the contamination of the ψ data from μ pairs produced upstream of the Fe is small and does not affect the results significantly. (A 60-cm hydrogen target was centered 60 cm upstream of the iron.)

The dimuon effective-mass ($M_{\mu\mu}$) spectra observed in 45 h of beam time are shown in Figs. 1(b) and 1(c). Only events which satisfied the reconstruction criteria discussed above and which had a total laboratory dimuon momentum, P_L, above 90 GeV are plotted. These data are

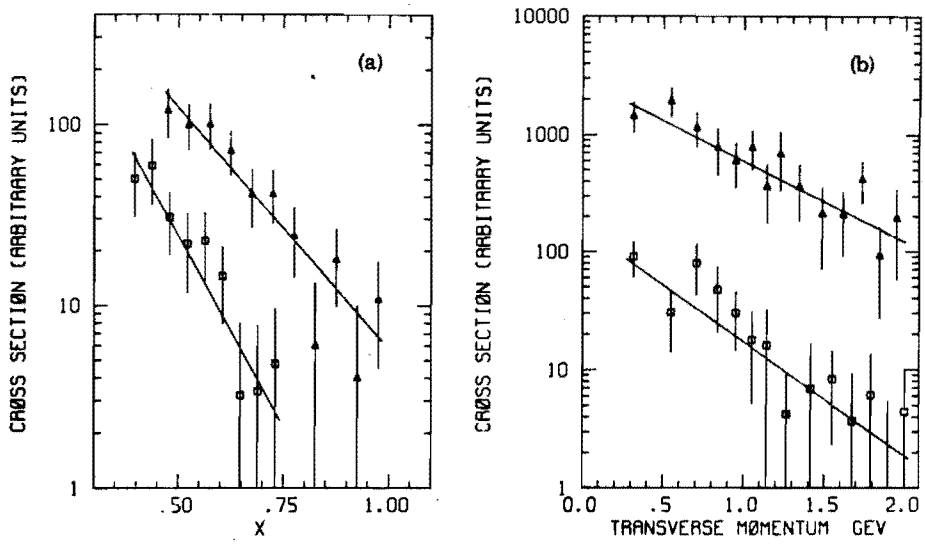

FIG. 2. (a) x distributions for pion (△) and proton (□) beams. For additional details, see text. (b) $P_\perp$ distributions for pion [(△), times 10] and proton (□) beams. For additional details see text.

not corrected for variation of spectrometer acceptance with mass. In the interval $2 \leq M_{\mu\mu} \leq 4$ GeV, the mass acceptance is a smooth structureless function of mass and varies by about ±35%. The low-mass regions of these spectra are presented as an indication of the overall μ-pair spectrum and will be discussed elsewhere. The dashed curves drawn in the region $M_{\mu\mu} \approx 3$ GeV represent the spectra calculated by a Monte Carlo method which takes into account the resolution and detection efficiency of the apparatus and assumes that all of the events in the interval $2.5 \leq M_{\mu\mu} \leq 3.7$ GeV, the ψ region, result from the decay $\psi \to \mu^+ + \mu^-$. In the ψ regions, we observe 104 and 45 events in the pion and proton data, respectively. An extrapolation of the data with $M_{\mu\mu} < 2.5$ GeV into the ψ regions indicates that the non-ψ contributions to the ψ regions are less than 20%. Since the agreement between the dashed lines and the data is good,[2] we interpret the observed enhancements as $\psi(3.1) \to \mu^+ + \mu^-$.

The acceptance-corrected distributions in $x \equiv P_L/P_B$ and dimuon transverse momentum, $P_\perp$, are shown in Figs. 2(a) and 2(b) for the ψ region. (In calculating the geometric acceptance, isotropy for the decay $\psi \to \mu^+ + \mu^-$ was assumed.) The solid lines are fits to the measured cross sections of the form

$$d^2\sigma/dx\,dP_\perp^2 \propto \exp(-ax - bP_\perp).$$

The results of the fits[3] are $a_\pi = 6.2 \pm 0.8$ and $b_\pi = 1.6 \pm 0.2$ GeV^{-1} for incident pions, and $a_p = 9.7 \pm 1.6$ and $b_p = 2.2 \pm 0.5$ GeV^{-1} for incident protons. We calculate that for both π's and p's, the effect of ψ production from secondaries produced in the Fe is negligible.

We have compared the yields of ψ mesons per incident π^-, Y_π, to the yield per incident p, Y_p. The ratio of the yields, $R = Y_\pi/Y_p$, is x dependent. For $x \geq 0.5$, $R = 7.4 \pm 2.0$, where the quoted error in R is dominated by the statistical uncertainty in Y_p. Systematic uncertainties in R are estimated to be significantly less than the statistical uncertainties and have been neglected. The fact that R is significantly greater than unity suggests that the mechanisms for ψ production at large x are basically different for π's and p's. This difference may indicate that the antiquark in the π^- plays a critical role in ψ production.

For a total Fe inelastic cross section of ~0.7 b, our data give, for $x \geq 0.5$, a total inclusive cross section for $\pi^- + \mathrm{Fe} \to \psi \to \mu^+ + \mu^-$ of ≈85 nb, ±50%, where the error is dominated by systematic errors. Previous results for ψ production by neutrons[4] of average energy 250 GeV from beryllium gave the probability per interacting neutron for $n + \mathrm{Be} \to \psi \to \mu^+ + \mu^-$, $|x| > 0.32$, as $P(n) = 0.43 \times 10^{-7}$ (quoted error of a factor of 2). Our result for protons from Fe for $x \geq 0.38$ is $P(p) = (0.59 \pm 0.30) \times 10^{-7}$ in reasonable agreement with the neutron result. The distributions in x and $P_\perp$ for the neutron data also appear consistent with our proton results.

We thank the Northeastern University Computa-

tion Center, the FNAL crew, and the FNAL fabrication procurement group for their support, and Brookhaven National Laboratory and Harvard University for the loan of equipment. We also thank B. Cairns, E. King, and D. Ronan for their help with this work.

---

*Accepted without review under policy announced in Editorial of 20 July 1964 [Phys. Rev. Lett. 13, 79 (1964)].

†Work supported in part by the National Science Foundation under Grant No. MPS70-02059A5.

‡Alfred P. Sloan Foundation Fellow.

[1]J. J. Aubert *et al.*, Phys. Rev. Lett. 33, 1404 (1975); J.-E. Augustin *et al.*, Phys. Rev. Lett. 33, 1406 (1974).

[2]If all ψ production were via $\psi'(3.7)$ production only $(7 \pm 4)\%$ of the yield in the ψ region of our data would be from $\psi'(3.7) \rightarrow \mu^+ + \mu^-$. This is based on the branching ratios from A. M. Boyarski *et al.*, Phys. Rev. Lett. 34, 1357 (1975), and J. A. Kadyk *et al.*, Lawrence Berkeley Laboratory Report No. 3687 (unpublished).

[3]Fits to $d^2\sigma/dx dP_\perp{}^2 \propto \exp(-b' P_\perp{}^2)$ give $b_\pi{}' = 0.81 \pm 0.14$ GeV^{-2} and $b_\psi{}' = 1.1 \pm 0.3$ GeV^{-2}.

[4]B. Knapp *et al.*, Phys. Rev. Lett. 34, 1044 (1975).

$\psi(3.1)$ PRODUCTION BY PIONS AND PROTONS AT FERMILAB*

G. L. Blanar, C. F. Boyer, W. L. Faissler, D. A. Garelick†, M. W. Gettner, M. J. Glaubman, J. R. Johnson, H. Johnstad, M. L. Mallary, E. L. Pothier, D. M. Potter, M. T. Ronan, M. F. Tautz, E. von Goeler and Roy Weinstein

Presented‡ by M. T. Ronan

Northeastern University at Boston
Boston, Massachusetts 02115

I will describe measurements of $\psi(3.1)$[1] meson production by pions and protons made by the Northeastern High Energy group at Fermi National Accelerator Lab, FNAL. I will give ψ production probabilities per inelastic collision, distributions in $X_L = P_{Lab}/P_{beam}$ and $P_\perp$, and the ratio of ψ yield per incident pion to that for protons as measured in the reactions

$$\pi^- + Fe \rightarrow \mu^+ + \mu^- + X \text{ at } P_{beam} = 200 \text{ GeV}$$

$$p + Fe \rightarrow \mu^+ + \mu^- + X \text{ at } P_{beam} = 240 \text{ GeV}$$

I will mention some features of the low mass region of our data. The di-muon data were taken during an experiment by our group which searched for charmed meson production in π^-p and pp interactions. I will not describe the charm search experiment at this time.

The experiment was performed in the M2 beam line in the Meson Lab at FNAL.[2] The M2 beam is nominally a diffractive proton beam since it views the meson area target at a production angle of 1.0 m rad; however, by reversing the polarity of the bending magnets, an intense π^- beam can be obtained at slightly lower energies. Beam hodoscopes were used to measure the incident beam particle's momentum to $\delta p_B/p_B \sim 0.2\%$, and its incident vertical and horizontal angles to $\delta\theta \sim 0.2$ m rad. The beam spot at the target was 1/4" x 1/4" and the

---

* Research supported in part by the National Science Foundation under grant MPS70-02059A5.

† Sloan Foundation Fellow.

‡ Invited paper at the 1975 SLAC Summer Institute on Particle Physics.

coordinates of the beam particle were measured to an accuracy of 1/16" horizontally and 1/8" vertically. Beam particle identification was accomplished using two threshold Cerenkov counters set on pions. The beam part of the trigger included signals from beam trigger counters and the absence of signals from halo veto counters. One of the beam counters was pulse height analyzed.

The data I will present was taken in a total of 45 hours of beam time. A 200 GeV negative pion (less than 1% kaon) beam was used for 25 hours at an intensity of $\sim 6.0 \times 10^5$ per $\sim .8$ sec pulse. For the remaining time we used a 240 GeV proton (less than .5% pion) beam at $\sim 7.5 \times 10^5$/pulse.

The apparatus used for the di-muon experiment was a solid iron μ spectrometer shown in Fig. 1. The μ-pairs were created at the front end of the first iron (Fe) absorber. Muons were identified by their traversal of 5.6 m of iron. A 60 cm hydrogen target, not shown, used for the charm search experiment was centered $\sim$ 60 cm upstream of the iron. The MP counters were used to determine the effect of upstream interactions. Counters M0 thru M5 were the di-muon trigger counters. The first $\sim$ 2.5 m of iron served as both target and hadron absorber. A 3 m long gapless iron magnet, assembled and wound by us, was used in conjunction with 3 magnetostrictive spark chambers to measure muon production angles and momenta. The proportional chamber was used only in checking the reconstruction technique and the spark chamber efficiencies for a subsample of the data.

The di-muon trigger required a six fold counter concidence, $M0 \cdot M1 \cdot (M2 \cdot M3) \cdot (M4 \cdot M5)$ in time with a beam particle trigger. The following steps were taken to insure that at least two muons passed through the apparatus: pulse heights 1 1/2 times minimum ionizing were required for M0 and M1 and a split counter coincidence,

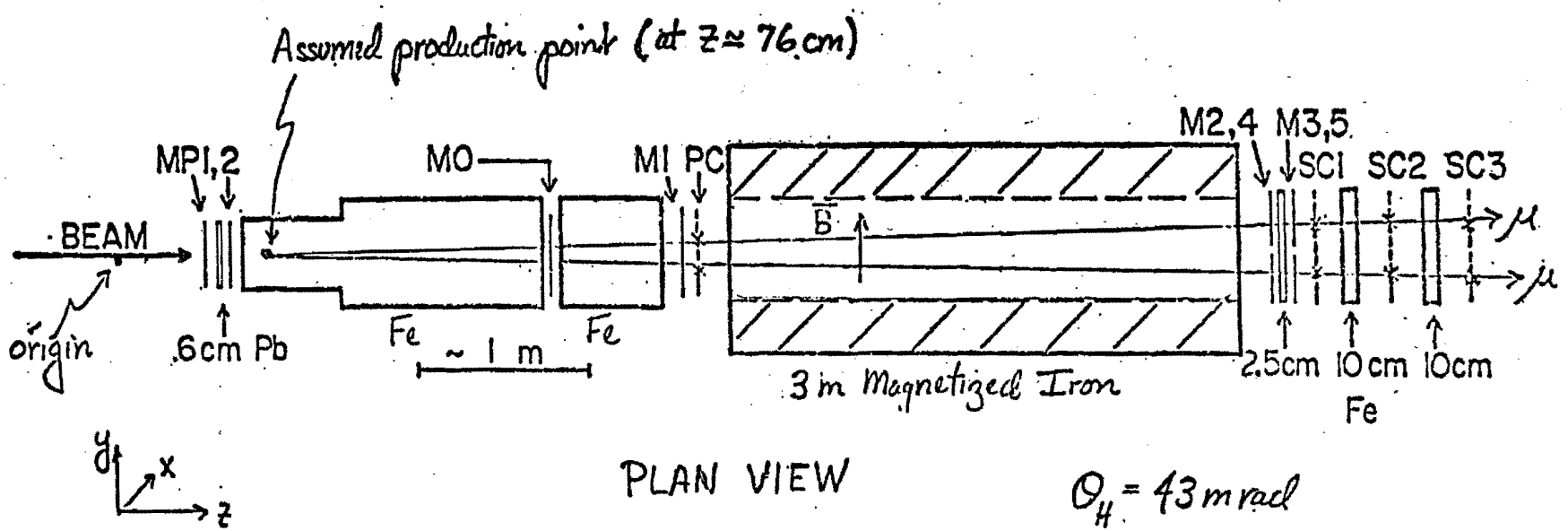

PLAN VIEW

$\theta_H = 43$ m rad

Fig. 1

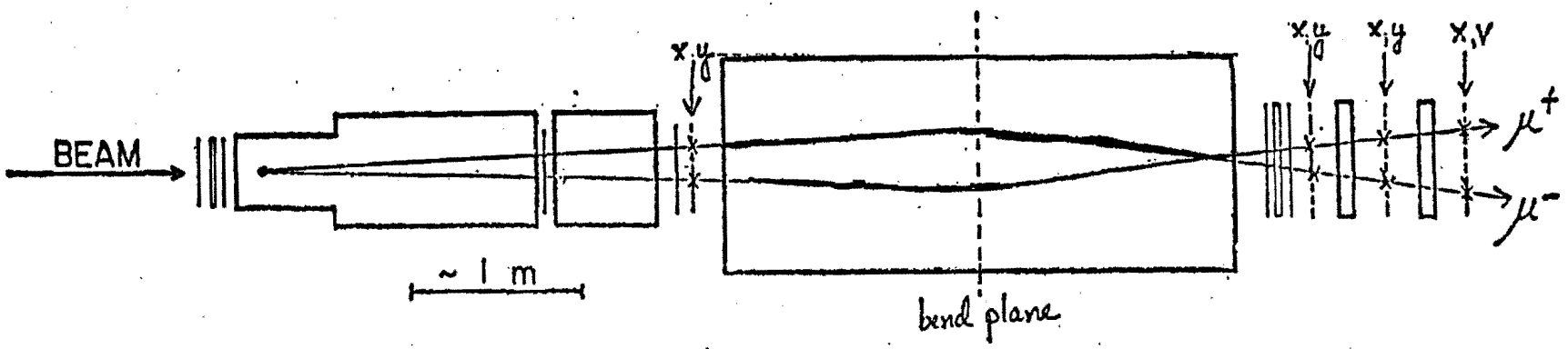

SIDE VIEW

$\theta_V = 32$ m rad

(M2·M3)·(M4·M5), was required at the rear of the magnet. Furthermore, iron was placed between the back trigger counters and between the spark chambers to eliminate backgrounds due to single muons which caused knock-on electrons. During the actual running we checked that there was no observable accidental component in the trigger. Also, we checked that the biases on the M0 and M1 counters were set well below the double minimum ionizing peak.

Alignments and magnet calibration were done using a μ beam. The M2 line is a two stage magnet system. In order to produce a μ beam, two collimators after the first stage were closed and the second stage was used to center the μ beam on a hodoscope just in front of the target. The momentum spectrum used to calibrate the iron magnet with 200 GeV muons is shown in Fig. 2. Superimposed are points obtained with a Monte Carlo program which simulates events in a model of our apparatus. The agreement is quite good. The calibration was checked at other values of the muon momentum. The magnetic field of the iron magnet was found in this way to be 18.5 Kilogauss. We have also found from an analysis of our wide opening angle events that the variation in average field over the active region of the magnet is less than 5%.

A study of the number of di-muon events, corrected for detection efficiency, per incident flux for a sample of the data runs checked the stability of the detector for the duration of the experiment.

The dimuon invariant mass, $M_{\mu\mu}$, was calculated from the tracks measured by the spark chambers, assuming the dimuon was produced inside the first iron absorber one absorption length from its edge along the beam line, at the point $z = 76$ cm in our coordinate system, see Fig. 1. The muon momenta and angles were reconstructed taking into account the bending and energy loss of the muons in the

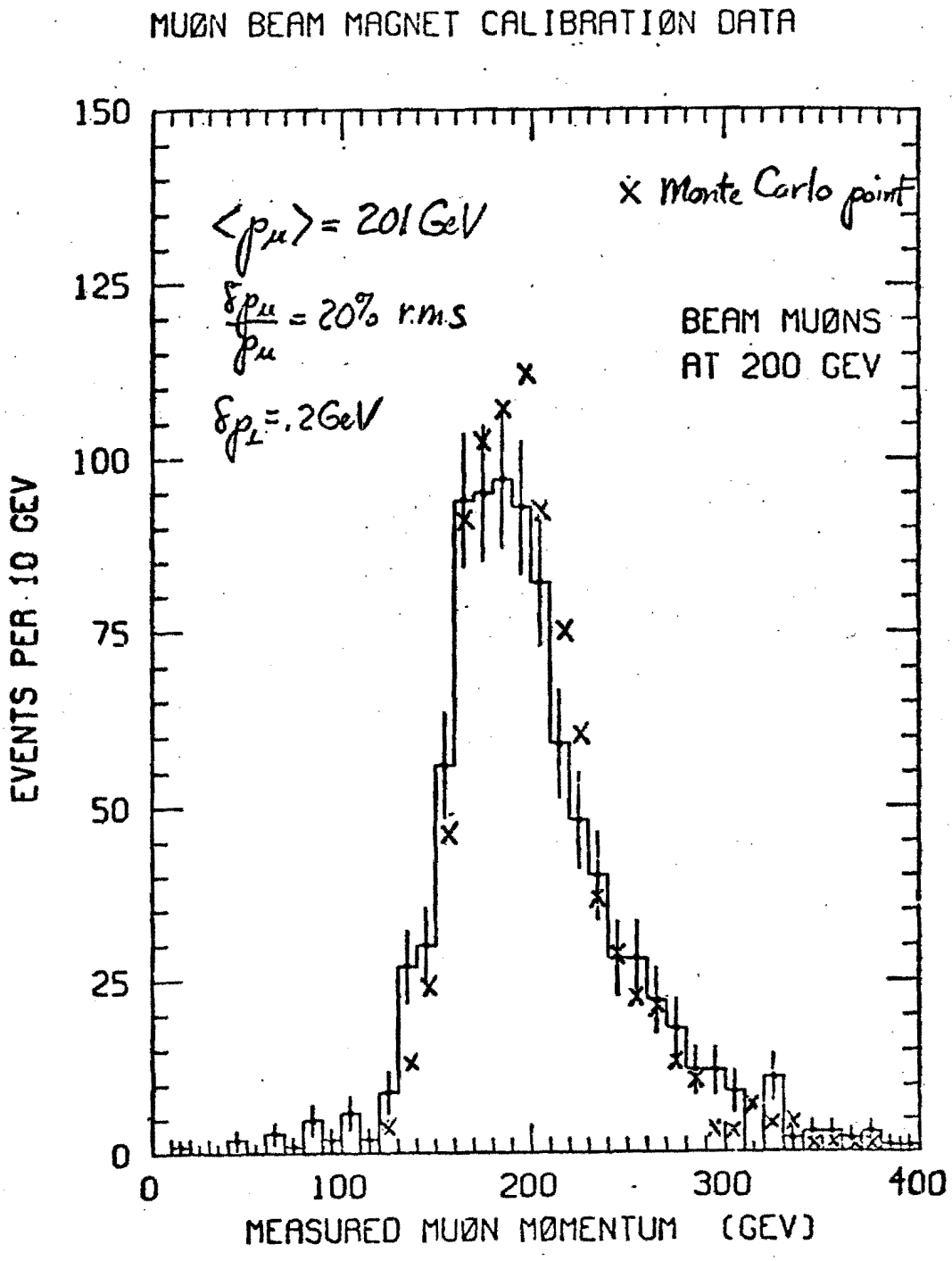
MUØN BEAM MAGNET CALIBRATIØN DATA
150
125
100
75
50
25
0
EVENTS PER 10 GEV
0
100
200
300
400
MEASURED MUØN MØMENTUM (GEV)
× Monte Carlo point
⟨pμ⟩ = 201 GeV
δpμ/pμ = 20% r.m.s
δpT = .2GeV
BEAM MUØNS
AT 200 GEV

Fig. 2

magnetized iron spectrometer.

Only $\mu^+\mu^-$ events were selected, eliminating $\approx$ 2% of the 2μ events. In the horizontal plane, where there is no bending, each muon track was extrapolated back to the assumed production point. The distribution of measured deviation at the production point divided by the expected standard deviation, calculated using the measured momentum of the track, was compared to a gaussian distribution, see Figs. 3 and 4. The discrepancy between the slope of .42 in Fig. 3 and the .5 one would expect for a gaussian distribution indicates an 8% error in our calculation of the expected standard deviation which is probably due to the fact that we neglected large angle Coulomb scattering. In the analysis, the tracks were required to deviate by less than 2.2 standard deviations removing $\approx$ 10% of the events. Note that we have placed the cut at a point near where the distribution for the pion beam data, Fig. 3, begins to deviate from the gaussian distribution; this deviation is peculiar to the pion beam data and we believe that it is due to a beam muon background.

For all of the data I will present we have required that the lab momentum of the di-muon be greater than 90 GeV; this insures that our acceptance for the events in the 3 GeV mass region is greater than $\sim$ 15%. For a fixed mass the acceptance of the apparatus is a smooth function of lab momentum, P_L, and transverse momentum, $P_\perp$. In the interval $2 \leq M_{\mu\mu} \leq 4$ GeV, the mass acceptance is a smooth structureless function of mass and varies by about $\pm$ 35%.

The dimuon effective mass spectra for the high mass region as observed are shown in Figs. 5 and 6. The dashed curves drawn in the region $M_{\mu\mu} \approx 3$ GeV represent the spectra calculated by a Monte Carlo method which takes into account the resolution and detection efficiency of the apparatus and assumes all of the events in the interval

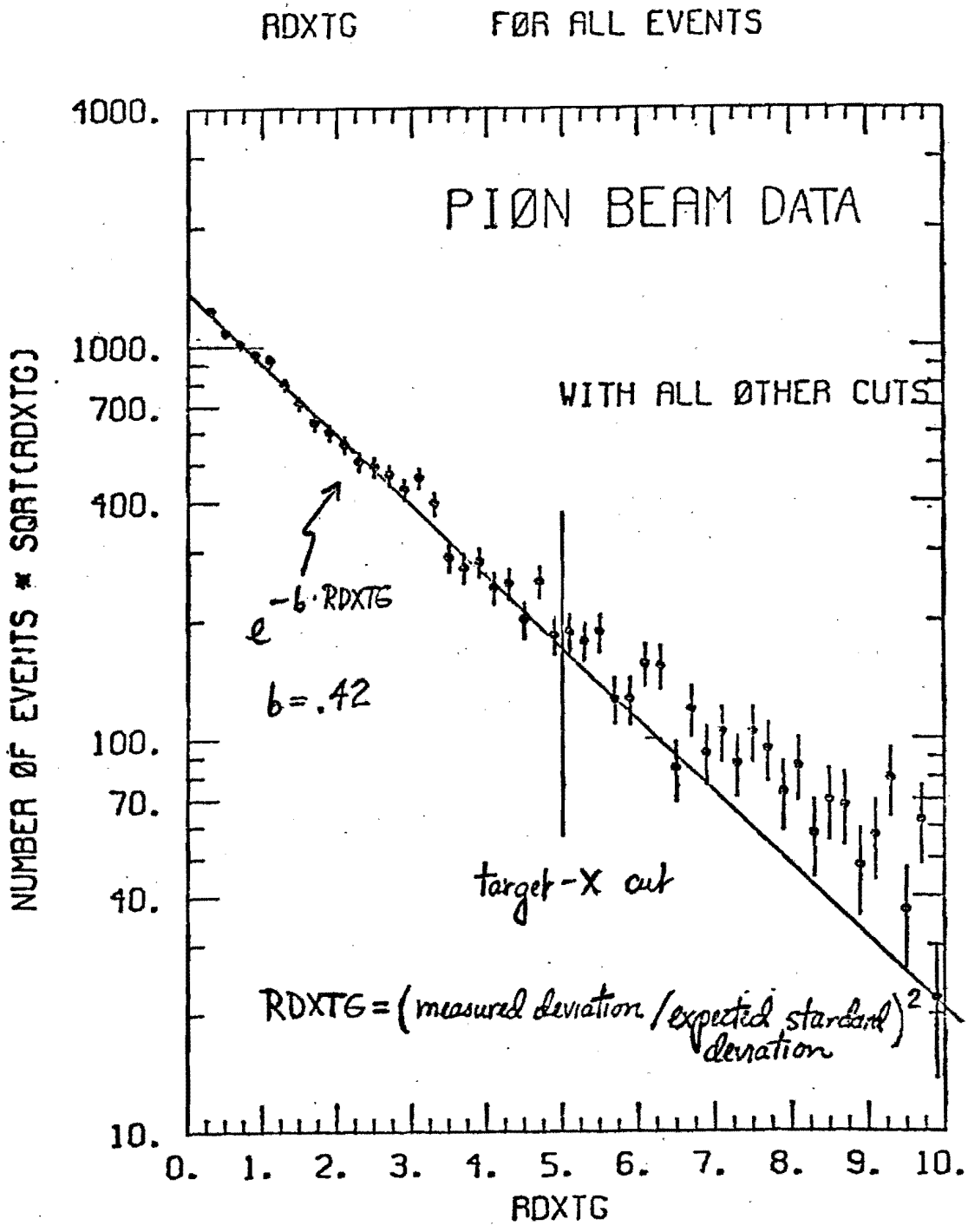
RDXTG FØR ALL EVENTS
PIØN BEAM DATA
WITH ALL ØTHER CUTS
NUMBER ØF EVENTS * SQRT(RDXTG)
1000.
700.
400.
100.
70.
40.
10.
$e^{-b \cdot RDXTG}$
b=.42
target-X cut
RDXTG = (measured deviation / expected standard deviation)^2
0. 1. 2. 3. 4. 5. 6. 7. 8. 9. 10.
RDXTG

Fig. 3

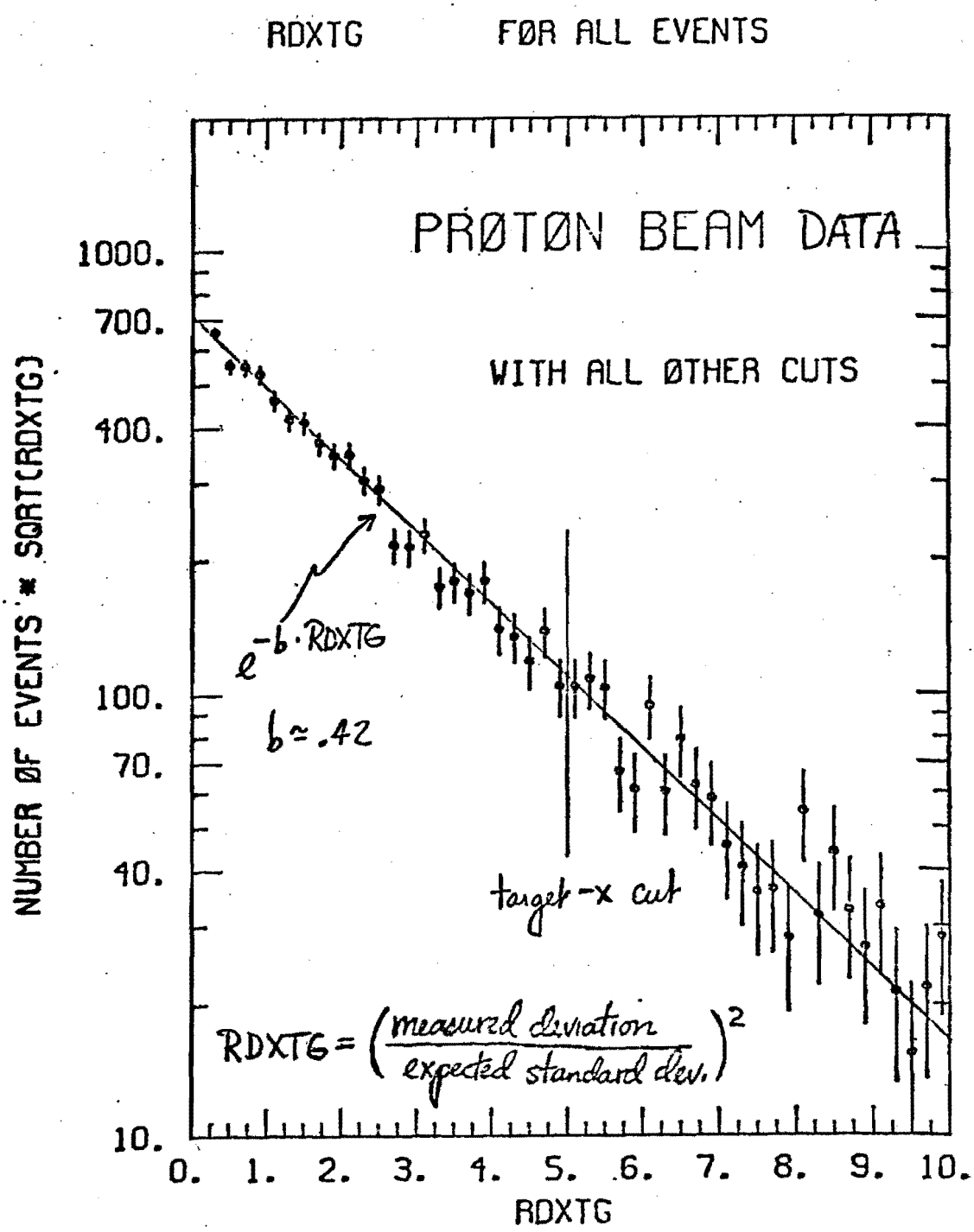
RDXTG FØR ALL EVENTS
PRØTØN BEAM DATA
WITH ALL ØTHER CUTS
NUMBER ØF EVENTS * SQRT(RDXTG)
1000.
700.
400.
100.
70.
40.
10.
0. 1. 2. 3. 4. 5. 6. 7. 8. 9. 10.
RDXTG
e^-b·RDXTG
b≈.42
target-x cut
RDXTG = (measured deviation / expected standard dev.)^2

Fig. 4

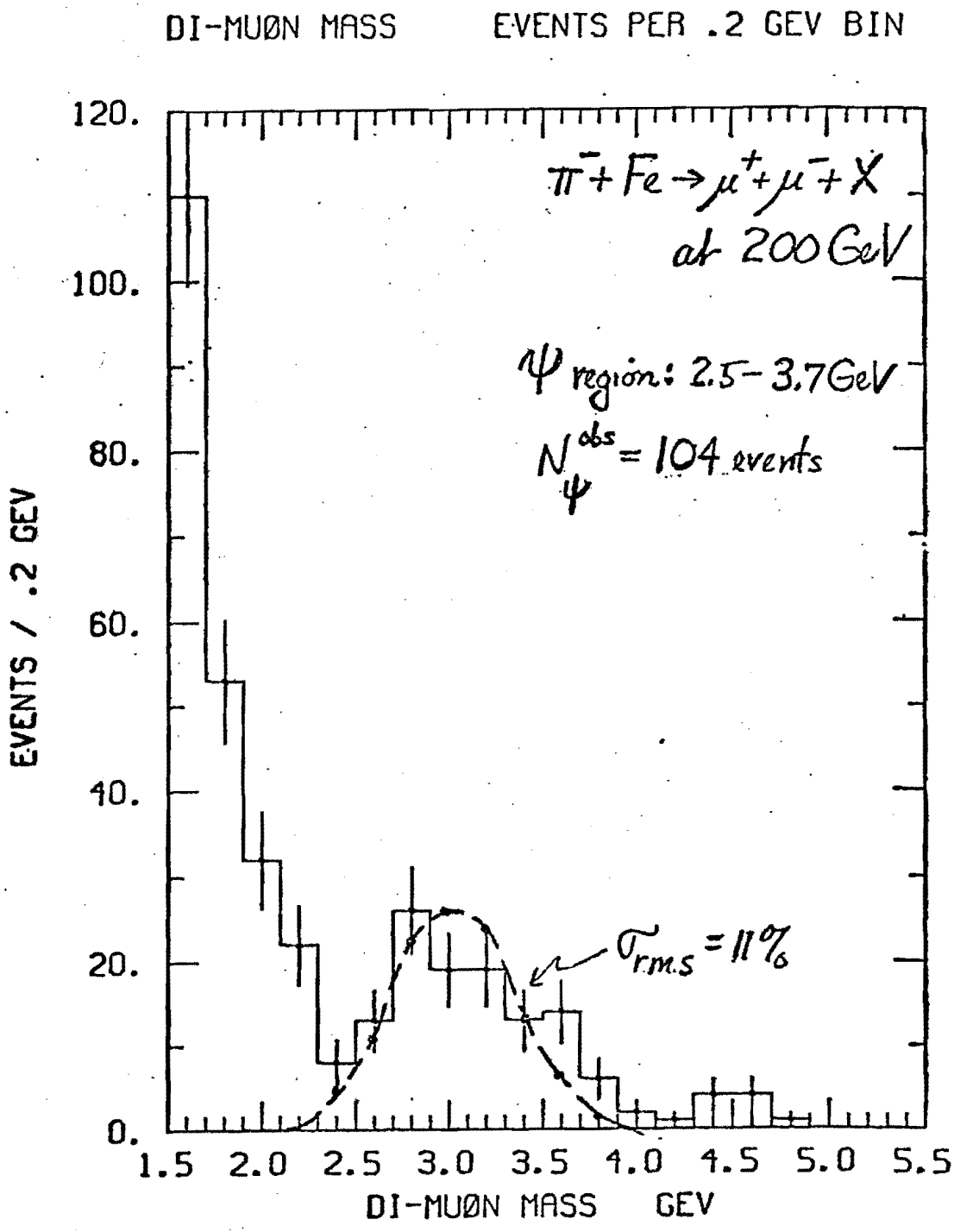
DI-MUØN MASS EVENTS PER .2 GEV BIN
$\pi^- + Fe \rightarrow \mu^+ + \mu^- + X$
at 200 GeV
ψ region: 2.5 – 3.7 GeV
$N_\psi^{obs} = 104$ events
$\sigma_{r.m.s} = 11\%$
EVENTS / .2 GEV
120.
100.
80.
60.
40.
20.
0.
1.5 2.0 2.5 3.0 3.5 4.0 4.5 5.0 5.5
DI-MUØN MASS GEV

Fig. 5

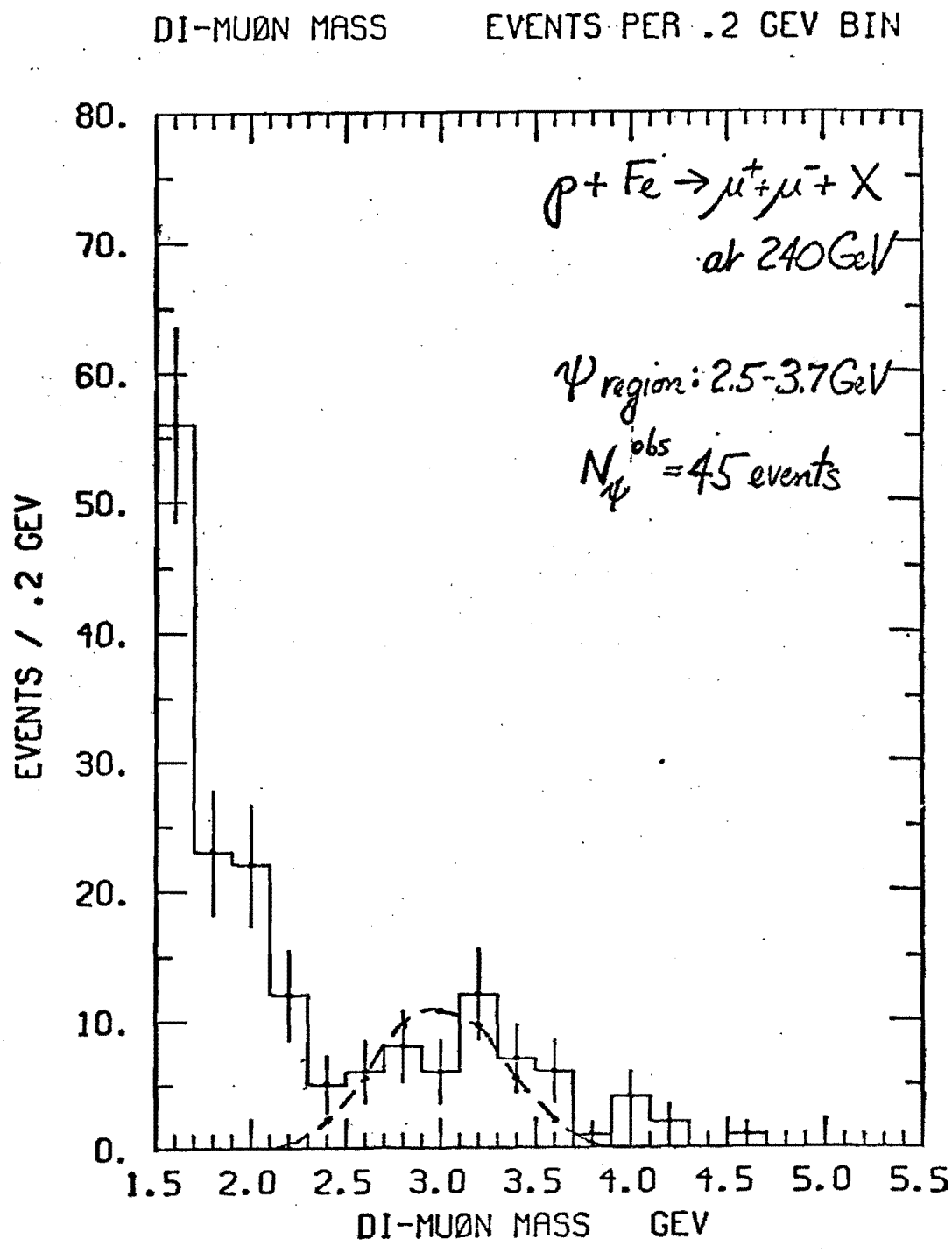
DI-MUØN MASS EVENTS PER .2 GEV BIN
$p + Fe \rightarrow \mu^+ + \mu^- + X$
at 240GeV
ψ region: 2.5-3.7GeV
$N_\psi^{obs} = 45$ events
EVENTS / .2 GEV
80.
70.
60.
50.
40.
30.
20.
10.
0.
1.5 2.0 2.5 3.0 3.5 4.0 4.5 5.0 5.5
DI-MUØN MASS GEV

Fig. 6

$2.5 < M_{\mu\mu} < 3.7$ GeV, the ψ region, result from the decay $\psi \rightarrow \mu^+\mu^-$. In the ψ region, we observe 104 and 45 events in the pion and proton data, respectively. Since the agreement between the dashed lines and the data is good, we interpret the observed enhancements as $\psi(3.1) \rightarrow \mu^+\mu^-$.

We have used the proportional chamber to check the source position for the events in the ψ region, $2.5 \leq M_{\mu\mu} \leq 3.7$ GeV. We consider only events which had a proportional chamber hit within 2 standard deviations of the calculated trajectory for each track. The proportional chamber hit and the position at the spark chambers were used to obtain a better measurement of the trajectory. The distribution of the z coordinate of the intercept in the horizontal plane of the two tracks is shown in Fig. 7. The resolution is poor but the mean is in good agreement with our assumed production point at z = 76 cm and the r.m.s. spread is in good agreement with Monte Carlo predictions.

We have chosen to present $X_L = P_{Lab}/P_{beam}$ and $P_\perp$ distributions corrected for the acceptance of the apparatus. To do this we wrote an event by event acceptance routine which assumes isotropic decay of the dimuon parent, neglects multiple scattering and uses a bend plane approximation to track through the magnet. To check this routine as well as to check all of our analysis routines we have generated Monte Carlo ψ events, let the muons multiple scatter and be accepted by a model of the apparatus, then corrected the events for acceptance. The resulting spectrum for a simulation of the X_L distribution for proton initiated ψ events, the distribution with the steepest slope, is shown in Fig. 8. There is reasonable good consistency; one can see the effect of the momentum resolution. We have checked that in all cases the disagreement between the best fit slope parameter and the generating parameter is less than the statistical errors for our measured slope parameters. Also, for the data, we have checked our

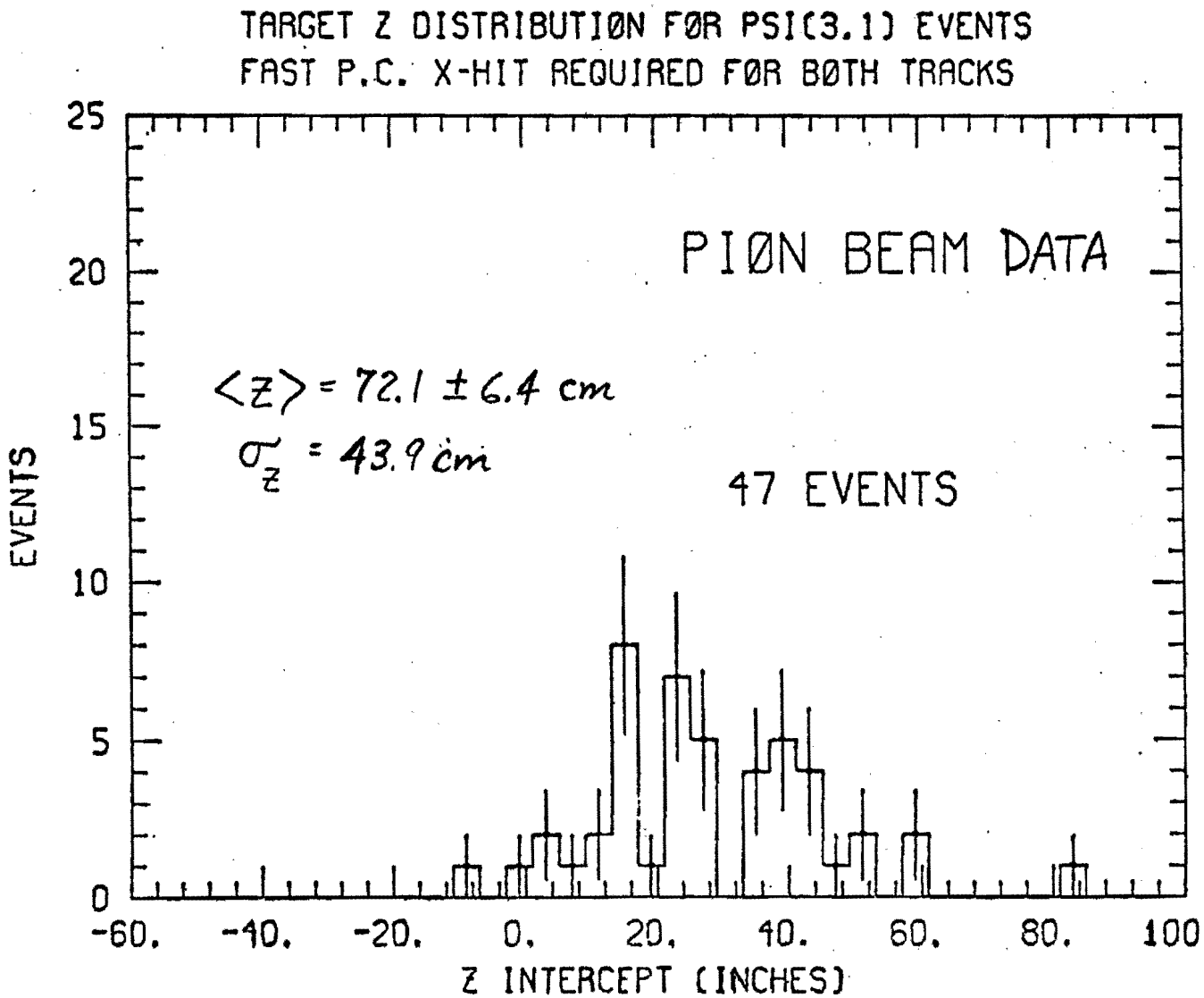
TARGET Z DISTRIBUTIØN FØR PSI(3.1) EVENTS
FAST P.C. X-HIT REQUIRED FØR BØTH TRACKS
PIØN BEAM DATA
⟨z⟩ = 72.1 ± 6.4 cm
σz = 43.9 cm
47 EVENTS
EVENTS
Z INTERCEPT (INCHES)
25
20
15
10
5
0
-60.
-40.
-20.
0.
20.
40.
60.
80.
100.

FIG. 7

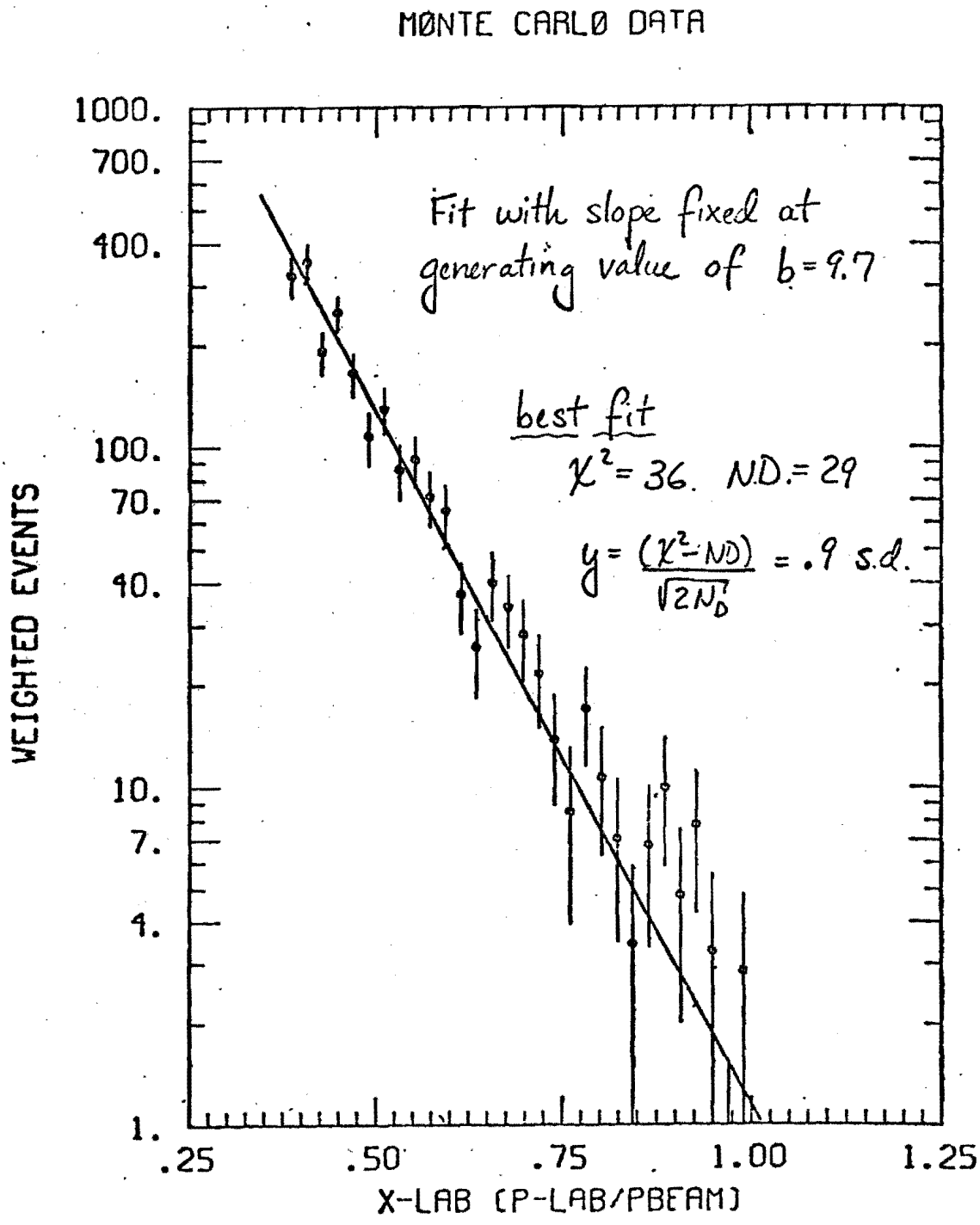
MØNTE CARLØ DATA
Fit with slope fixed at generating value of b=9.7
best fit
χ^2= 36. N.D.= 29
$y = \frac{(\chi^2 - ND)}{\sqrt{2N_D}}$ = .9 s.d.
WEIGHTED EVENTS
1000.
700.
400.
100.
70.
40.
10.
7.
4.
1.
.25
.50
.75
1.00
1.25
X-LAB (P-LAB/PBEAM)

Fig. 8

fitted slope parameters against parameters obtained by fitting the uncorrected data directly using the Monte Carlo program.

The acceptance corrected distributions in X_L and $P_\perp$ for events in the ψ region are shown in Figs. 9 and 10. The solid lines are fits to the measured cross section of the form:

$$d^2\sigma/dX_L dP_\perp^2 \alpha \exp(-aX_L) \times \exp(-bP_\perp)$$

The results of the fits are for incidents pions $a_\pi = 6.2 \pm 0.8$ and $b_\pi = 1.6 \pm 0.2$ $(GeV)^{-1}$, and for incident protons $a_p = 9.7 \pm 1.6$ and $b_p = 2.2 \pm 0.5$ $(GeV)^{-1}$.

We have calculated using measured branching ratios of the $\psi'(3.7)$[3] that less than $7. \pm 4.\%$ of the yield in the ψ region, $2.5 \leq M_{\mu\mu} \leq 3.7$ GeV, is from $\psi'(3.7) \rightarrow \mu^+\mu^-$. From an extrapolation of a power law fit to the low mass data we find $\sim 5\%$ of the pion data and $\sim 3\%$ of the proton data in the ψ region is associated with the low mass region of our data, see Figs. 11 and 12. We are still analyzing the high mass data, $M_{\mu\mu} > 3.7$ GeV, and will try to understand the mass spectrum of events associated with these events and possible extrapolations into the ψ region. We calculate using π and γ inclusive spectra from πp and pp interactions, the measured ψ photoproduction cross section[4] and our own measured pion ψ production cross section and X_L distributions that the background in our pion and proton beam data due to secondaries is less than 6%. Using doubly charged data ($\mu^+\mu^+$ and $\mu^-\mu^-$), we find the background due to π and K decay is less than 2%. We are presently analyzing muon beam particle backgrounds but we believe this background to be negligible for the proton beam data and less than 10% for the pion beam data.

Using the MP counters, see Fig. 1, we have determined that our results are independent of whether or not we require a single minimum ionizing particle in the first counter. We chose not to cut on the

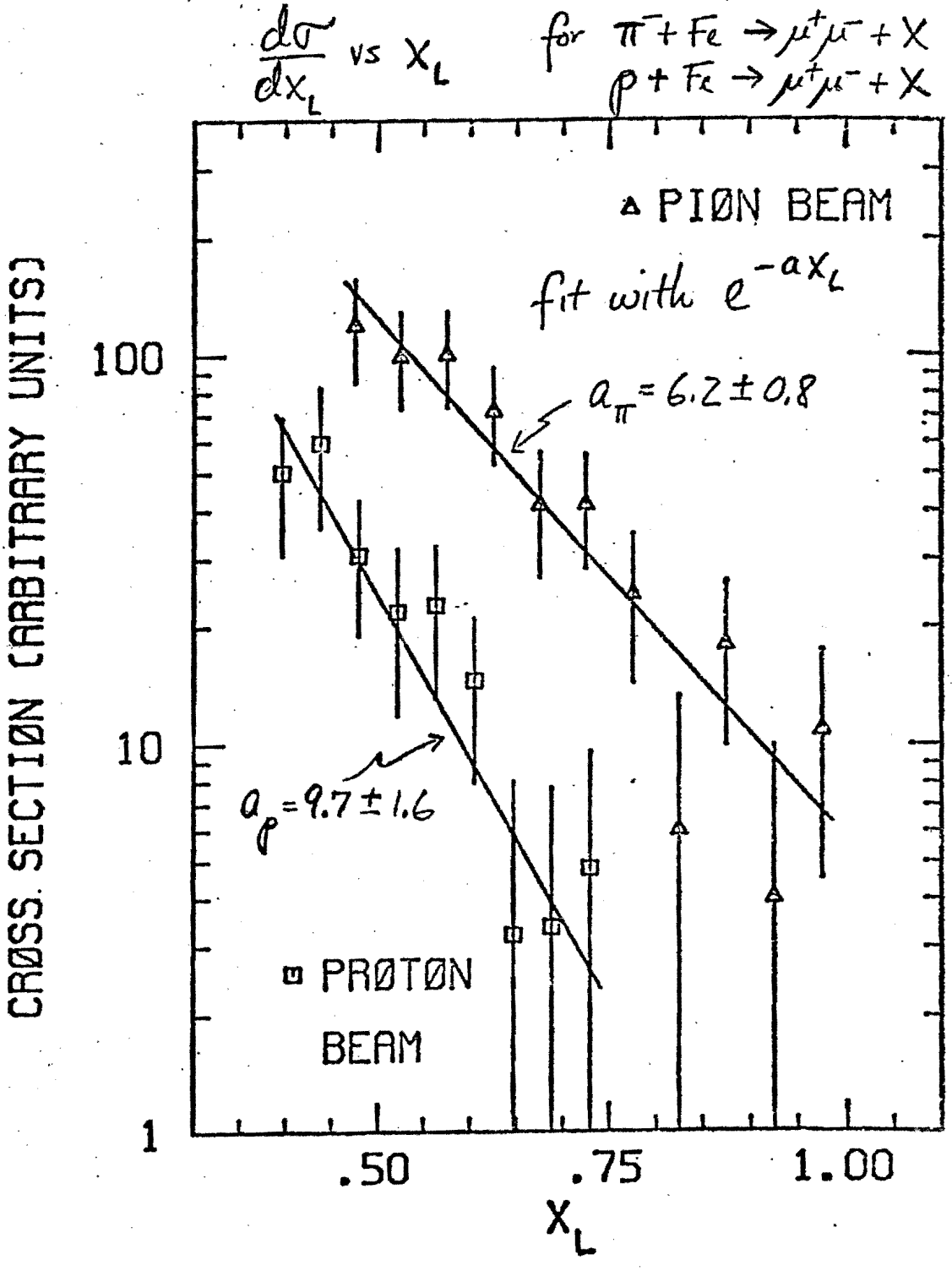
$\frac{d\sigma}{dx_L}$ vs X_L
for $\pi^- + Fe \to \mu^+\mu^- + X$
$p + Fe \to \mu^+\mu^- + X$
▲ PIØN BEAM
fit with e^{-aX_L}
$a_\pi = 6.2 \pm 0.8$
$a_p = 9.7 \pm 1.6$
□ PRØTØN BEAM
CRØSS SECTIØN (ARBITRARY UNITS)
100
10
1
.50
.75
1.00
X_L

Fig. 9

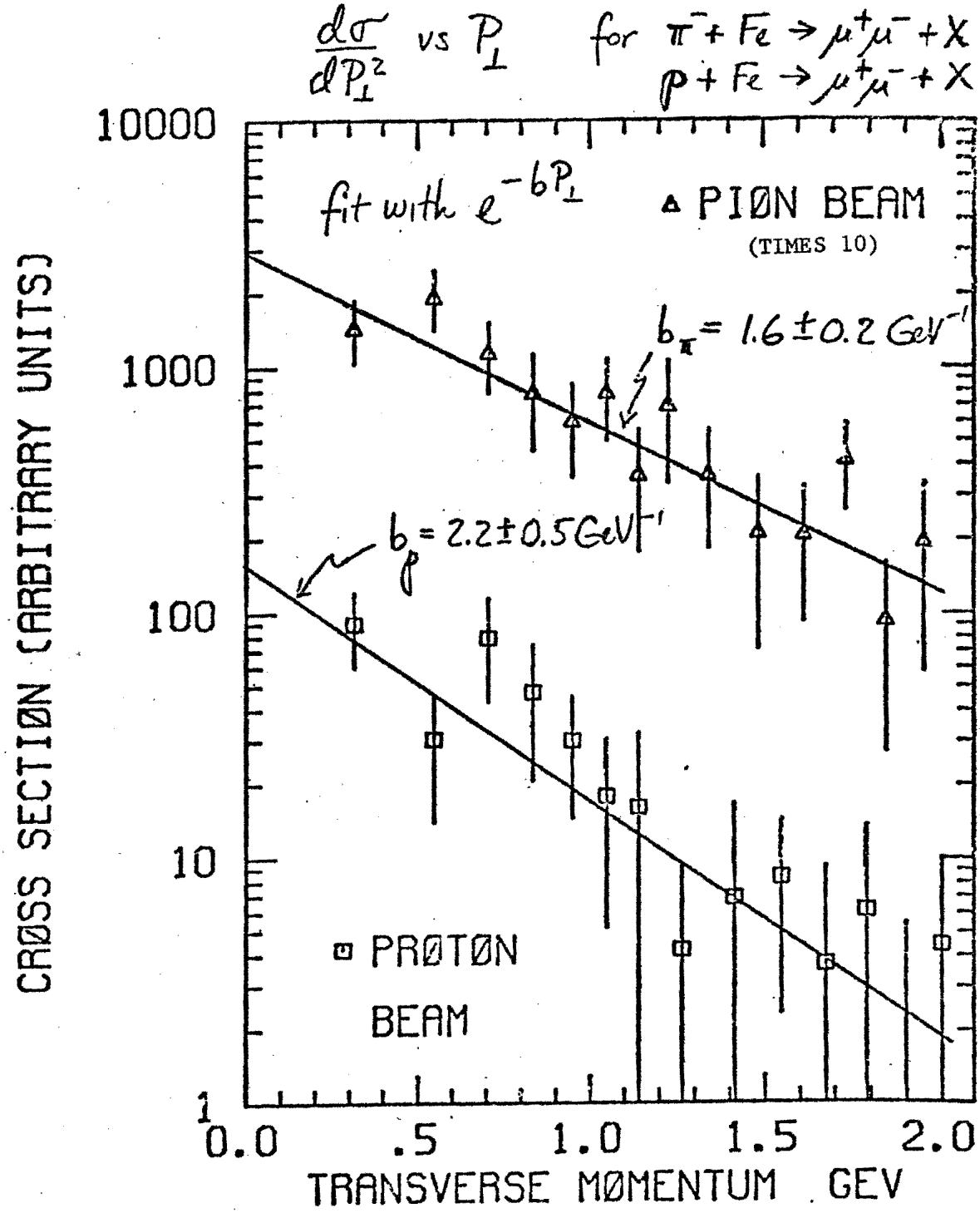
$\frac{d\sigma}{dP_\perp^2}$ vs $P_\perp$ for $\pi^- + Fe \to \mu^+\mu^- + X$
$p + Fe \to \mu^+\mu^- + X$
fit with $e^{-bP_\perp}$
▲ PIØN BEAM
(TIMES 10)
$b_\pi = 1.6 \pm 0.2\ GeV^{-1}$
$b_p = 2.2 \pm 0.5\ GeV^{-1}$
□ PRØTØN BEAM
CRØSS SECTIØN (ARBITRARY UNITS)
10000
1000
100
10
1
0.0
.5
1.0
1.5
2.0
TRANSVERSE MØMENTUM GEV

Fig. 10

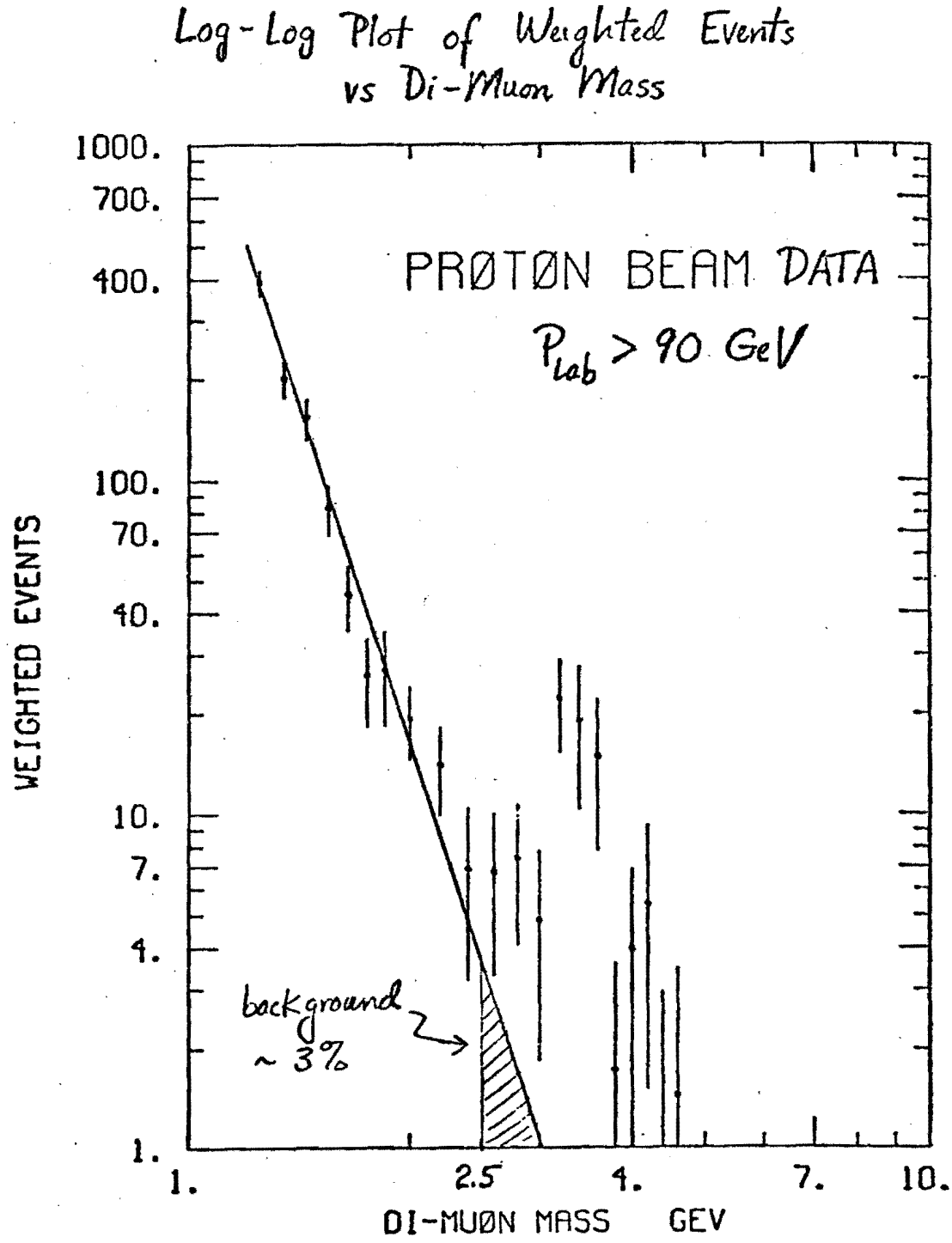
Log-Log Plot of Weighted Events
vs Di-Muon Mass
PRØTØN BEAM DATA
$P_{lab} > 90$ GeV
background
~ 3%
WEIGHTED EVENTS
1000.
700.
400.
100.
70.
40.
10.
7.
4.
1.
1.
2.5
4.
7.
10.
DI-MUØN MASS GEV

Fig. 11

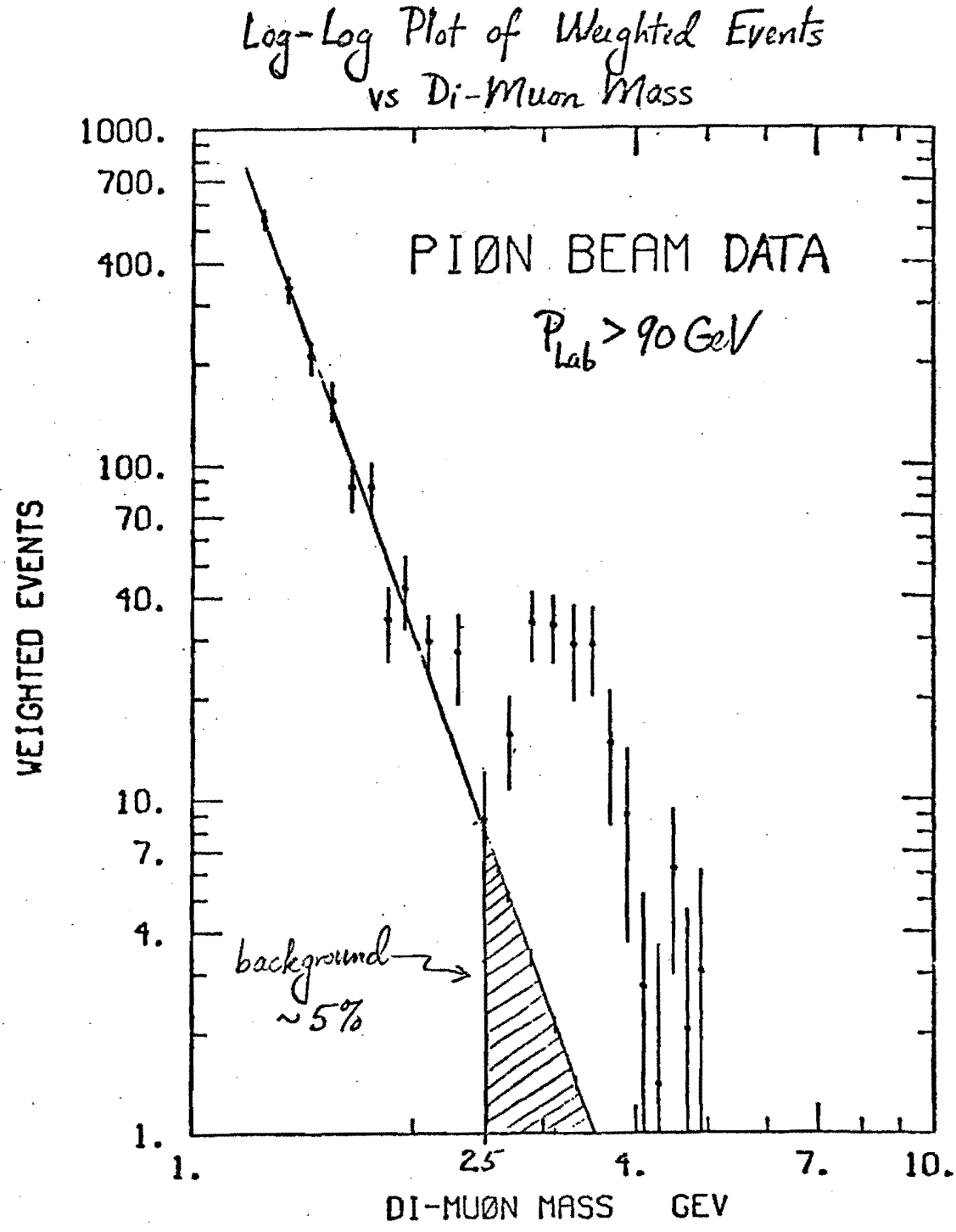
Log-Log Plot of Weighted Events
vs Di-Muon Mass
PIØN BEAM DATA
$P_{Lab} > 90$ GeV
WEIGHTED EVENTS
1000.
700.
400.
100.
70.
40.
10.
7.
4.
1.
background
~5%
1.
2.5
4.
7.
10.
DI-MUØN MASS GEV

Fig. 12

MP counters to avoid possible biases. We calculate that ~ 5% of our pion beam data and ~ 8% of our proton beam data may be associated with ψ production in the H_2 target.

We use the observed number of produced ψ's, corrections for detection efficiency, acceptance and target-X cut losses to calculate ψ production probabilities. At the present stage of analysis the backgrounds appear small. We have not done any background subtractions. We calculate the probability of producing a ψ per inelastic interaction in iron times the branching ratio into $\mu^+\mu^-$ to be:

$$P_\pi(\psi) = (1.58 \pm .79) \times 10^{-7}, \quad X' > .45$$

$$P_p(\psi) = (.59 \pm .30) \times 10^{-7}, \quad X' > .375$$

where the errors are an estimated $\pm$ 50% systematic error, and where we have used $X' \equiv X_L = P_{Lab}/P_{beam}$. We compare to the results of ψ production by neutrons on a Beryllium target[5] by calculating the implied production probabilities and comparing at the same X'_{min}, see Fig. 13. We find good agreement in slope but a factor of 4 discrepancy in normalization.

We have compared the yield of ψ mesons per incident π^-, Y_π, to the yield per incident p, Y_p. The ratio of the yields, $R = Y_\pi/Y_p$, is X'_{min} dependent. For $X' \geq .5$, $R = 7.4 \pm 2.0$, where the quoted error in R is dominated by the statistical uncertainty in Y_p. The fact that R is significantly greater than unity suggests that the mechanisms for ψ production at large X' are different for pions and protons. This difference may indicate that the antiquark in the π^- plays a critical role in ψ production.

For a total Fe inelastic cross section of ~ .7 barns our data gives for

$\pi^- Fe \rightarrow \psi \rightarrow \mu\mu$ $\quad \sigma B = 109 \pm 55$ nanobarns for $X' > .45$

$pFe \rightarrow \psi \rightarrow \mu\mu$ $\quad \sigma B = 41 \pm 21$ nanobarns for $X' > .375$

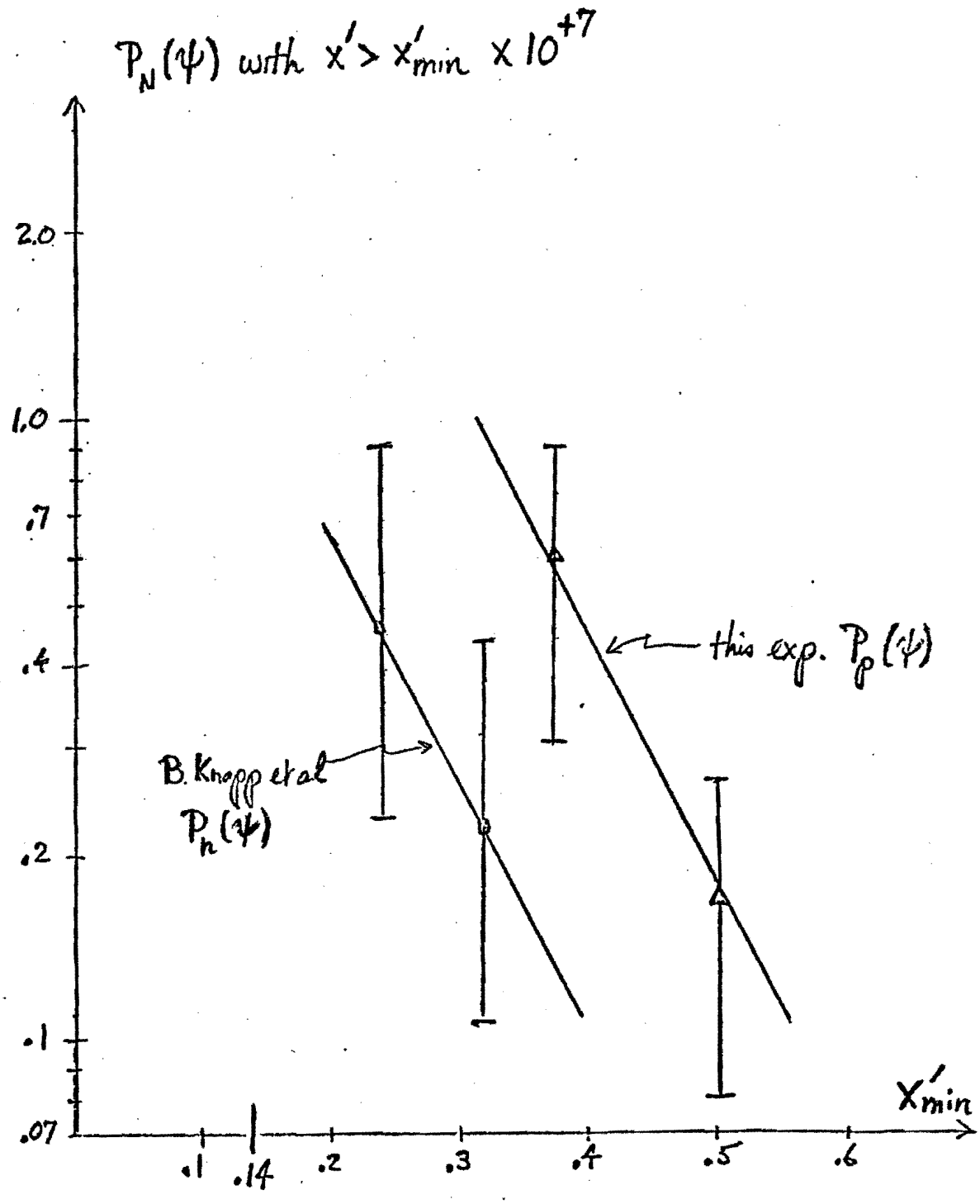
$P_N(\psi)$ with $x' > x'_{min} \times 10^{+7}$
2.0
1.0
.7
.4
.2
.1
.07
.1
.14
.2
.3
.4
.5
.6
x'_{min}
B. Knapp et al
$P_n(\psi)$
this exp. $P_p(\psi)$

Fig. 13

Using inelastic cross sections of 32 mb for pp and 21 mb for πp, neglecting absorption of the ψ in the Fe nucleus ($\approx$ 5% effect) and using the branching ratio of ψ into $\mu\mu$ [3] we find

$$\sigma_{\pi N}(\psi) \simeq 48 \pm 24 \text{ nanobarns/nucleon, } X' > .45$$

$$\sigma_{pN}(\psi) \simeq 27 \pm 14 \quad " \quad " \quad X' > .375$$

Extrapolating to X' = .14, assuming no break in slope, multiplying by 2 for production in the forward and backward hemisphere, we estimate that the total ψ production cross section in proton nucleon collisions is $\approx .54 \pm .36$ microbarns.

In Figs. 14 and 15 I show the dimuon effective mass spectra for all events, which satisfy the criteria discussed earlier, for the pion and proton beam runs. These data are not corrected for variation of spectrometer acceptance with mass. I would like to point out only a few features of the low mass, $M_{\mu\mu} < 2.5$ GeV, region of our data since we are still analyzing them. First, there is a general similarity in shape of the two mass spectra and an overall factor of $\sim$ 2.5 higher yield by pions compared to the yield by protons even though the data is cut at a higher X' for the pion beam data than for the proton beam data (X'_{min} is .45 for the pion beam data and .375 for the proton). Secondly, there is a peak in the mass spectrum at $\approx$ 700 MeV which may or may not be entirely inclusive ρ^o production.

We have corrected the data for acceptance in the region $1.2 \leq M_{\mu\mu} \leq 2.5$ GeV, see Figs. 11 and 12 and have found a M^{-n} dependence with $n \approx 6$ for both the pion and proton beam data. We have also compared the yield per incident pion to that per incident proton above the same X'_{min}. We find for X' > .5, $R(\pi/p) \simeq 4.7$ compared to $R(\pi/p) = 7.4 \pm 2.0$ for the ψ region. These facts may suggest that dimuons in the $1.2 \leq M_{\mu\mu} \leq 2.5$ GeV mass region are produced by the same process by which ψ's are produced and that the basic interactions by

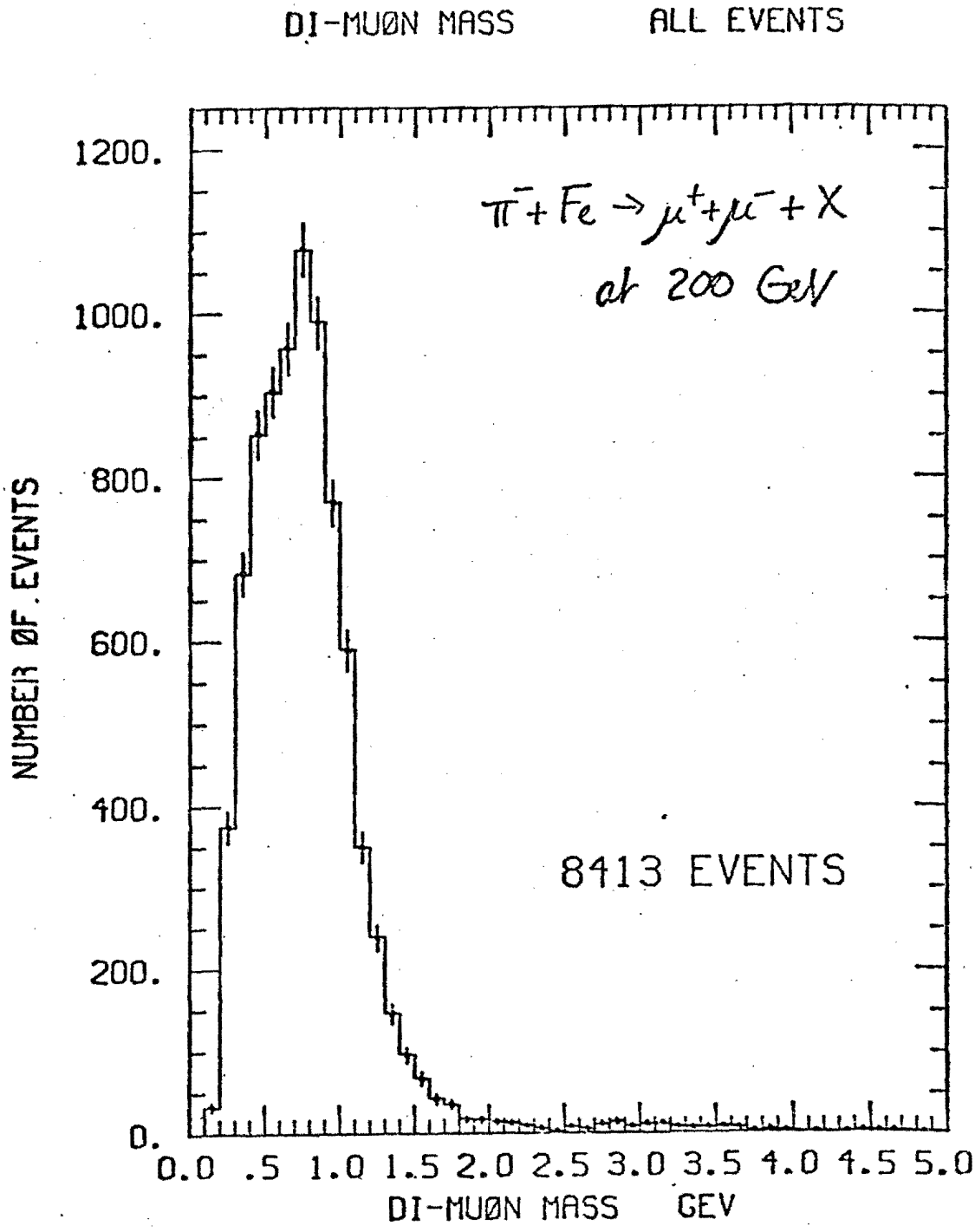
DI-MUØN MASS ALL EVENTS
$\pi^- + Fe \rightarrow \mu^+ + \mu^- + X$
at 200 GeV
8413 EVENTS
NUMBER ØF EVENTS
1200.
1000.
800.
600.
400.
200.
0.
0.0 .5 1.0 1.5 2.0 2.5 3.0 3.5 4.0 4.5 5.0
DI-MUØN MASS GEV

Fig. 14

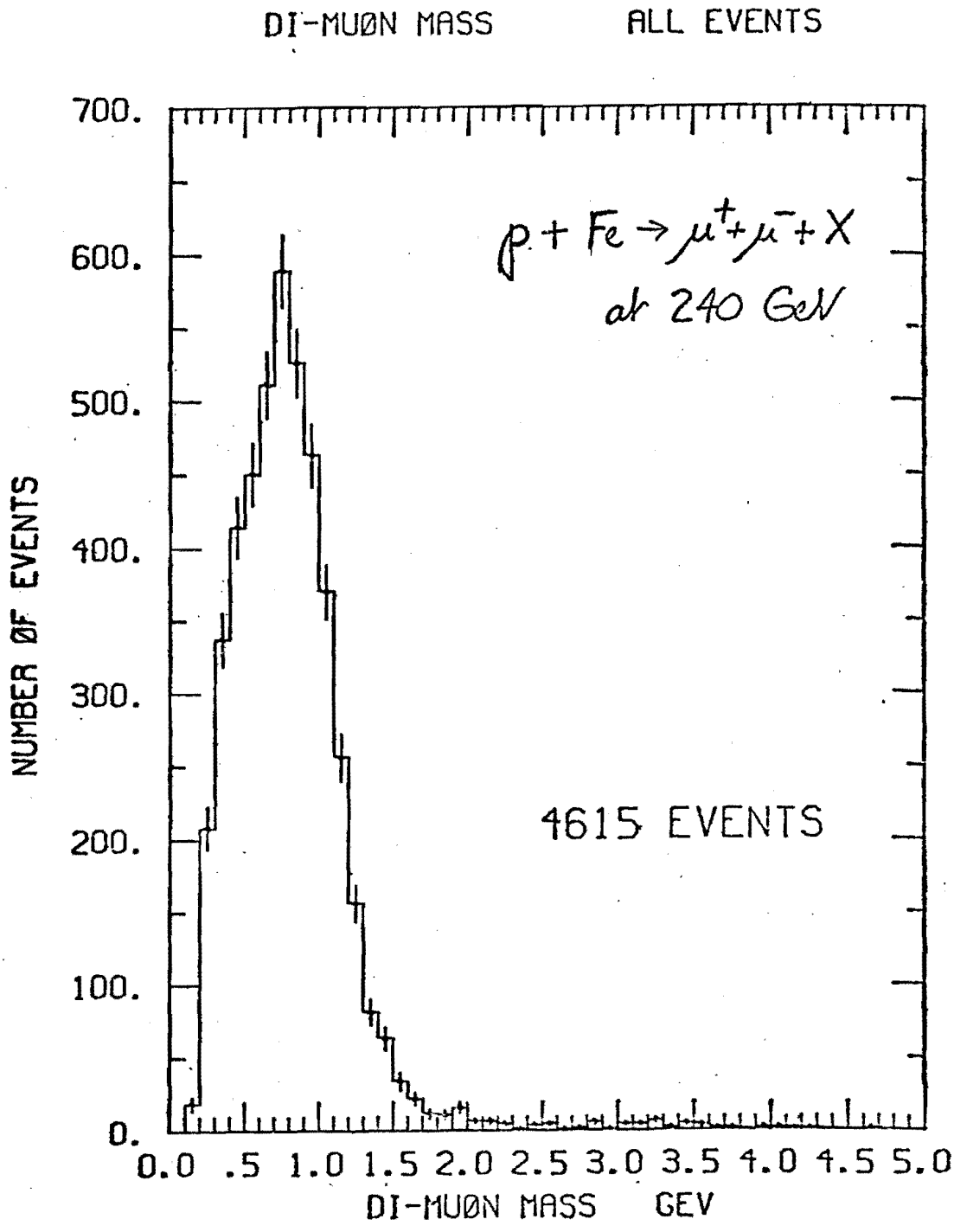
DI-MUØN MASS ALL EVENTS
$p + Fe \rightarrow \mu^+ + \mu^- + X$
at 240 GeV
4615 EVENTS
NUMBER ØF EVENTS
700.
600.
500.
400.
300.
200.
100.
0.
0.0 .5 1.0 1.5 2.0 2.5 3.0 3.5 4.0 4.5 5.0
DI-MUØN MASS GEV

Fig. 15

which pions and protons produce dimuons are similar but differ in strength. Finally, I would like to remind you that we are still analyzing the low mass region and have not completely understood apparatus effects in the measurement of these data in that region.

REFERENCES

1. J. J. Aubert, et al., Phys. Rev. Lett. 33, 1404 (1975) and J. E. Augustin, et al., Phys. Rev. Lett. 33, 1406 (1975).

2. This report gives in more detail results previously reported, G. Blanar, et al., Phys. Rev. Lett. 35, 346 (1975).

3. A. M. Boyarski, et al., Phys. Rev. Lett. 34, 1357 (1975) and J. A. Kadyk, et al., LBL report #3687 (unpublished).

4. B. Knapp, et al., Phys. Rev. Lett. 34, 1040 (1975).

5. B. Knapp, et al., Phys. Rev. Lett. 34, 1044 (1975).